Simulated rockburst experiment: Development of a numerical model for seismic wave propagation from the blast, and forward analysis

by M.W. Hildyard* and A.M. Milev†

Synopsis

A blast was engineered close to a tunnel in a deep-level mine with the purpose of studying the wave interaction with the tunnel. Numerical modelling of seismic wave propagation was used in both the forward planning and the back-analysis of this experiment. This paper presents the forward analysis. A likely model for a propagating blast was investigated and developed. This model predicts the influence of the velocity of detonation of the blast and the rise-time of the blast on the radiation pattern, and hence on the expected positions of maximum velocity at the tunnel surface. An attempt was made to quantify the parameters of the blast model, using waveform data from two other blast experiments. The blast model caused particle velocities which were an order of magnitude lower than these measured velocities. Large values for blast pressure were required to match the amplitudes of the recorded velocities. An alternative 'effective' source with a similar mechanism but increased diameter was proposed to account for the higher velocities. It was established that distant velocities scale with the square of the borehole diameter. A calibration blast at the experimental site was also modelled. Agreement in the waveforms was not sufficient for conclusive statements to be made about the validity of the source model. However, the modelled waveforms show an encouraging correspondence with some measured waveforms. This gave confidence that the model could be used to examine wave propagation around the tunnel, and allowed a scaled source to be developed for forward analysis of the main experiment.

Introduction

An artificial rockburst experiment was performed in an underground mine tunnel (Hagan *et al.*[1]). The purpose was to create a controlled seismic event, which could be closely monitored, and to induce and observe damage in a nearby tunnel. The experiment used a large blast at a distance from the tunnel to generate the incident seismic waves.

Extensive numerical modelling of seismic wave propagation was used in both the forward and back analysis of this experiment. Modelling was used to give insight into the design of the experiment, the blast and the positioning of monitoring equipment. The experiment was attractive as potential data against which models of wave propagation around excavations could be developed and evaluated. In particular, the source position and size were well known, monitoring equipment was close to the source and tunnel surfaces, and positions of damage were well known. This is generally not the case with natural rockbursts.

This work describes the forward analysis for the experiment leading to projections of wave propagation from the blast and of the wave motions around the tunnel. Modelling the wave propagation is naturally very dependent on the source. Although the position and size of the blast were well known, the mechanism of the source was not well understood. The experiment used long blastholes with a finite detonation velocity, parallel to the tunnel, to generate the incident seismic waves. The blasthole lengths were large relative to the distance to the tunnel, so the source process needed to be modelled. A significant amount of the forward analysis had to be devoted to developing models of wave propagation from a propagating blast.

The paper proposes a source model, and compares a numerical implementation of the source with analytic results. The effects of the various parameters of this source are then studied. Waveforms from blast recordings are examined to determine appropriate values for the source parameters. Comparisons are presented between the model and waveforms from a calibration blast, recorded at various positions along the experimental tunnel. The calibration data is used to project values of source parameters for the experiment, and results of applying the source to a model of the tunnel experiment are presented.

* *CSIR: Division of Mining Technology, Auckland Park, South Africa and Department of Earth Sciences, University of Liverpool, United Kingdom.*

† *CSIR: Division of Mining Technology, Auckland Park, South Africa.*

 SA ISSN 0038–223X/3.00 + 0.00. Paper received Feb. 2001; revised paper received Aug. 2001.

Models were implemented using a finite difference program WAVE (Cundall[2], Hildyard *et al.*[3]). The geometry of the experiment was such that it fitted in with the orthogonal limitations of the program (i.e. the tunnel was approximately square, and the blastholes were approximately parallel to the tunnel). In describing this work three different 'velocities' are frequently used, namely (i) The velocity of propagation of detonation—generally referred to as VOD (velocity of detonation), (ii) The velocity of seismic wave propagation, referred to as the 'wave-speed' and (iii) The velocity of particle motion (or ground motion), simply referred to as 'velocity'.

Source model for a propagating blast

The experiment used explosives in boreholes to create the seismic event. The boreholes had charge lengths from 4 to 7 m, diameters of 0.1 m, and were 5 to 7 m from the tunnel. The size of the source was therefore comparable to the distance to the area of interest and could not be modelled by a far-field approximation. The detonation speed of the blast was comparable to the elastic wave-speeds of the rock-mass. In this paper this is referred to as a 'propagating' blast to differentiate it from an 'instantaneous' blast.

A conceptual model of a propagating blast is an advancing ring of pressure along the inside of a cylindrical cavity, Parnes[4]. A detailed review of previous analytical investigations is presented by Daehnke[5] and Kouzniak and Rossmanith[6]. Numerical simulations of this model using two-dimensional axisymmetry were presented by Daehnke[5], Rossmanith *et al.*[7] and Uenishi *and Rossmanith*. Among the findings, it should be noted that shear waves are developed due to the non-uniform loading of the surface. When the velocity of detonation (VOD) is less than the P-wave speed (C_P), the shear wave is dominant. It was shown that three different cases should be distinguished depending on the detonation velocity: supersonic (VOD > C_P), transonic (C_S < VOD < C_P), and subsonic (VOD < C_S). Recently, Kouzniak and Rossmanith[6] presented analytical expressions for the time-varying stress and displacement components at any distance from the wall of an infinite borehole in the supersonic case, for various shapes of applied loading.

For our application a source was required which would model stress waves emanating from a propagating blast in a borehole to a distance hundreds of times larger than the borehole diameter, but of the same order as the length of charge. A three-dimensional numerical model with our volume of interest required as coarse as possible a representation of the source to be developed. It was found that this model could be accurately implemented, without representing the borehole surface. This is important as it simplifies the representation of the source, and relaxes the fineness of the numerical discretization which would be required to model a cylindrical cavity. Instead, pressure is propagated along a line in the solid material of a finite difference mesh. This is not a superposition of point sources, as a point along the line is not influenced by neighbouring points.

The source model consists of applying dilatational pressure ($\sigma_1=\sigma_2=\sigma_3$) along a line of grid-points within the solid material of a finite difference mesh. The charge-length and diameter are directly related to the length of the line and the grid-point spacing in the finite difference implementation. Larger diameters are modelled by pressurizing parallel lines or a volume of grid-points. In this case enclosed grid-point calculations are disabled. The pressure function describes how the pressure at a point in the source varies with time. The phase of this pressure function varies along the charge line. The velocity of detonation is then the rate at which this pressure function is propagated along the line of grid-points. The source was implemented on a staggered finite difference grid. For this implementation, a single grid-point source-width corresponds to an equivalent circular borehole diameter of 1.27 times the grid-point spacing.

The accuracy of this implementation of the proposed model was established by comparing waveforms from this numerical source, with those obtained using the analytical expressions of Kouzniak and Rossmanith[6], when VOD / C_P = 2.23. The radial stresses at distances of 2 and 100 borehole radii are compared in Figure 1 for a smooth-step pressure function (the pressure function describes the variation of pressure at a point with time). The numerical waveform corresponds closely to the analytic result, except for a known problem of numerical dispersion at high frequencies. The numerical oscillations can be removed using smaller element sizes or a smoother pressure function. Indeed it should be noted that the shape used for the pressure function is not smooth in its second derivative, yet was used to make the analytic problem tractable, at the expense of some undesirable high frequency in the numerical model. Further comparisons of the numerical and analytical waveforms are given in a more general non-dimensional form in Kouzniak and Rossmanith[6]. The analytical expressions are valid only for the supersonic case. The numerical model allows any detonation velocity, so it can be expected and is assumed, that good comparisons for the supersonic case imply that the numerical implementation is accurate for the subsonic and transonic cases.

Characteristics of the propagating blast source

There are six controllable parameters in the source model: the charge-length, the diameter, the velocity of detonation, and the pressure function, which in turn is controlled by the pressure shape-function, the rise-time and the peak-pressure. Models were investigated to establish the effect of

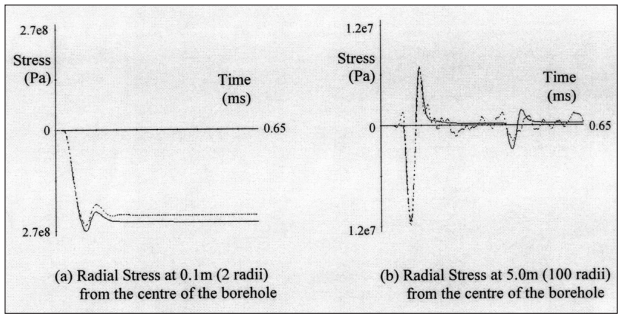

Figure 1—Comparison of a coarse numerical solution (dotted line) with the analytical solution (solid line), for a propagating smoothed step load along the borehole wall. The source and elastic properties are: borehole diameter 0.1 m, pressure rise-time 83 μs, peak pressure 1 GPa, velocity of detonation (VOD) 12000 m/s, P-wave velocity (C_p) 5370 m/s, S-wave velocity (C_S) 3287 m/s, with VOD = 2.23 C_p

each of these parameters on the amplitude and wave-type composition at a distance from the source.

Velocity of detonation (VOD)

The velocity of detonation has a very significant influence on the amplitudes, the wave-types and the angles of the wave-fronts generated. The significance of detonation velocity is relative to the P- and S-wave speeds of the material. An increase in material wave-speeds has an effect equivalent to decreasing the source detonation velocity.

Figure 2 compares waves emanating from the propagating blast model for three different detonation velocities: an infinite detonation velocity or instantaneous source, a detonation velocity just above the P-wave speed, and a detonation velocity between the P- and S-wave speeds. The instantaneous source predominately produces a P-wave with a cylindrical wavefront parallel to the source. S-waves are only produced from diffraction at the blast edges. In contrast, the propagating source produces both P-waves and S-waves. The S-wave component increases relative to the P-wave component for lower detonation velocity. The wavefronts are conical and the angle of the wavefront also depends upon the detonation velocity. For a detonation velocity close to the wave-speed, the wavefront becomes normal to the axis of the source, while for a detonation velocity much higher than the wave-speed the wavefront is parallel to the axis of the source.

Figure 3 shows the radiation patterns for different detonation velocities, as represented by the maximum velocities at varying positions around the source. Comparing Figures 3a, b, and c shows that for a lower detonation velocity:

- ➤ Maximum velocities are reduced
- ➤ The angle of the wavefront becomes more normal to the source
- ➤ The lobes of maximum velocity shift increasingly ahead of the source.

The effect of detonation velocity becomes less important for shorter lengths of charge or longer rise-times (longer wavelengths), i.e. as the ratio of charge-length to wavelength decreases. This occurs because the wavefronts from a greater percentage of the source overlap.

Charge length (L)

The charge length can be expected to influence amplitudes, wavelength and the distance at which far-field assumptions hold true. The effect of varying charge length was not studied here, as it is one parameter in the source model which corresponds directly to the physical source.

Borehole diameter (D)

It was found that, for the range of interest, the velocity amplitudes are approximately proportional to the square of the borehole diameter. Figure 4 compares radiation patterns for different diameters, where the pressure has been adjusted by the inverse of the square of the diameter (D^{-2}) giving approximately equal amplitudes. Figure 5 shows this relationship more clearly, by comparing the velocities at a point 8 metres ahead of the centre of the borehole, and 4 metres normal to it (marked 'H' in Figure 4), for two different source diameters. The relationship was found to hold approximately both for closer and further distances.

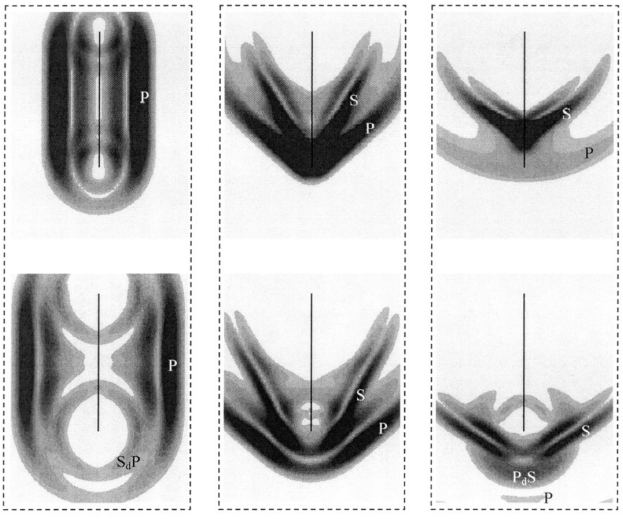

(a) C_D infinite (Instantaneous) (b) C_D = 7000 m/s (122% C_P; 199%C_S) (c) C_D = 4000 m/s (70% C_P; 144%C_S)

Figure 2—Comparison of the positions of P- and S-wavefronts for three different detonation velocities (VOD), as shown by snapshots of particle velocity. A subscript 'd' indicates a diffracted wave. The different cases show that the VOD:C_s ratio affects the angles of the wavefronts and the relative strengths of P- and S-waves. For slower detonation velocities, the wavefronts become more normal to the line of the source and the S-wave amplitude increases relative to the P-wave amplitude. (Values for detonation velocity should be seen relative to wave-speeds in the model which were C_p = 5740 m/s, and C_s = 3510 m/s)

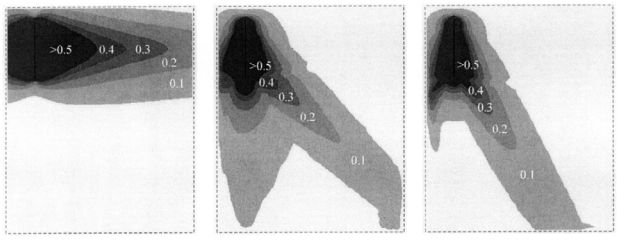

(a) (b) (c)

Figure 3—Effect of detonation velocity (VOD) on radiation pattern and amplitudes, expresses through contours of maximum velocity (m/s). The detonation direction is downwards. The effect of detonation velocity is relative to the wave-speeds of the material, which are C_P = 5740 m/s and C_S = 3510 m/s. All sources have a 400 μs rise-time, a 0.25 m diameter, an 8 m long borehole and a peak pressure (P) of 1 GPa. (a) Instantaneous source (infinite VOD) (b) VOD = 5000 m/s (c) VOD = 4000 m/s

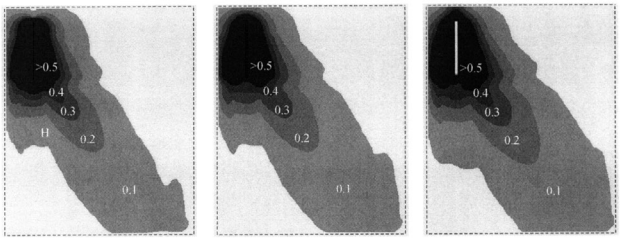

(a) (b) (c)

Figure 4—Effect of borehole diameter (D) on radiation pattern and amplitudes, expressed by contours of maximum velocity (m/s). All sources have a 800 μs rise-time, and a 8 m long borehole. Diameters are in the ratio 1:2:4, with peak pressures in the ratio 1:$^1/_4$:$^1/_{16}$ (a) D = 0.25 m, P = 3.33 GPa (b) D = 0,5 m, P = 0.833 GPa (c) D = 1.0 m, P = 0.208 GPa

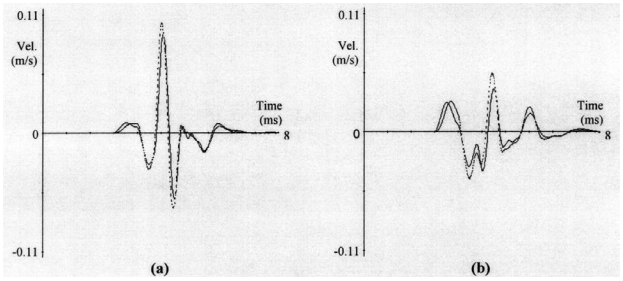

Figure 5—Effect of source diameter. Velocity waveforms at position 'H' in Figure 4, for different diameters and peak pressures. The solid line is for D = 0.25 m, P = 3.33 GPa, while the dashed line is for D = 1.0 m, P = 0.208 GPa—i.e. diameters are in the ratio 1:4, with peak pressures in the ratio 1:$^{1}/_{16}$. (a) X-velocity, normal to line of source (b) Z-velocity, parallel to line of source

Pressure function (shape)

Typically, blasts cause a rise in displacement to some maximum and then decay to a non-zero final displacement due to permanent deformation and fracturing around the source (Denny and Lane[9], Donze and Magnier[10]). In our model we control the blast pressure, which is applied as a smooth step function and does not return to zero so as to account for the permanent deformation. The pressure is held at its peak to keep the resulting waveforms as simple as possible, although a decay to some lower but non-zero value is more realistic. Figure 6 shows the shape of the pressure function used, its first and second derivative, and the frequency spectrum of the second derivative. The case of load applied uniformly to a spherical cavity is presented in Timoshenko and Goodier[11]. Analysing their expressions, we note that if the applied pressure is smooth and slow relative to the sphere dimension, then the velocity waveforms in the far-field tend to the second derivative of the applied pressure, while those very close to the source correspond to the first derivative. Although a pressure propagating along a line is a more complicated source, the above gives a starting point for controlling the frequency content.

The shape of the pressure function has an influence on frequency. A shape, virtually identical to the shape used but with a smoother second derivative, contains less high frequency and is better behaved numerically. The shape shown in Figure 6 was used to allow a broader range of frequency. Figure 7 compares the radiation patterns for the chosen source shape, an alternative smooth step, and a smooth pulse, all with the same rise-time to peak pressure. These source wave-shapes are shown in Figure 8. In these cases, the slope to peak pressure is relatively constant, in which case the pressure rise-time is of greater influence than the shape.

Peak pressure

For linear elastic models the velocity at any point is proportional to the peak pressure.

Pressure rise-time (T).

The rise-time (T) is defined here as the time from the initial rise to the peak pressure. The pressure decay is generally much more gradual and is ignored as it has little influence on the seismic waves. The frequency content (Figure 6d) is decreased if the pressure rise-time is increased. Comparing the radiation patterns for different source rise-times (Figure 9), shows that increasing the rise-time decreases the extent to which lobes of maximum velocity are shifted ahead of the

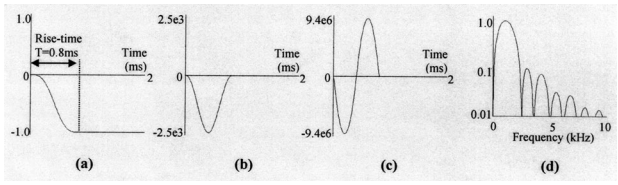

Figure 6—The pressure function characteristics. (a) Shape and rise-time of the pressure function (GPa) (b) First time derivative of the pressure function (GPa/s) (c) Second time derivative of the pressure function (GPa/s^2) (d) Frequency spectrum (relative amplitude) of the second derivative (GPa/s)

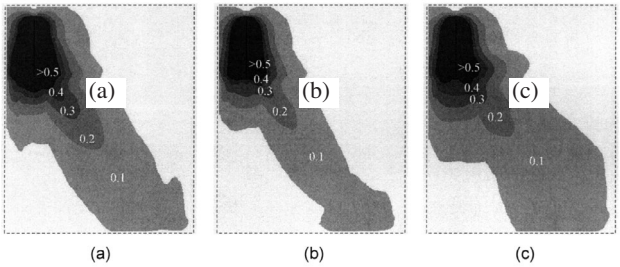

Figure 7—Effect of pressure function (shape) on radiation pattern and amplitudes, expressed by contours of maximum velocity (m/s). All sources have a detonation velocity of 4000 m/s, a 0.25 m diameter, an 8 m long borehole, and a peak pressure of 3.33 GPa. (a) Smooth step (used throughout Figures 2 to 6, and 9) (b) Alternative smooth step (c) Smooth pulse. All rise-times to peak pressure are 800 μs, and source shapes are shown in Figure 8

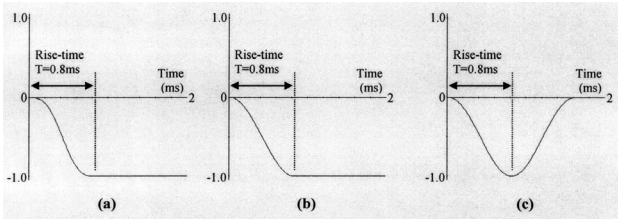

Figure 8—Pressure function wave-shapes as used in the models for Figure 7. All sources have equal rise-times, with pressure in GPa, (a) Smooth step (b) Alternative smooth step (c) Smooth pulse

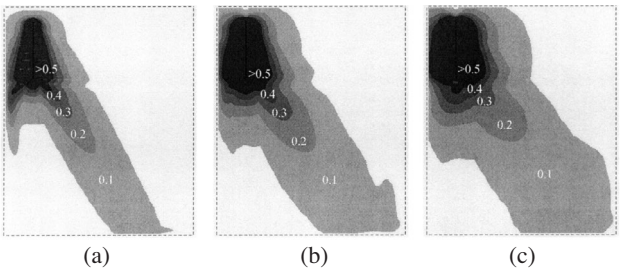

Figure 9—Effect of pressure rise-time (T) on radiation pattern and amplitudes, expressed by contours of maximum velocity (m/s). All sources have a VOD of 4000m/s and a 0.25 m diameter, 8 m long borehole. (a) T = 400 μs, P = 1.67 GPa (b) T = 800 μs, P = 3.33 GPa (c) T = 1200 μs, P = 6.67 GPa

source. This is opposite to the effect of a slower detonation velocity. Amplitudes decrease significantly for longer rise-times. For the pressure shape and the range shown here, the amplitude is approximately related to T^{-1}.

Calibration with data from blasts

Comparison with physical data was important to estimate parameters for the source model, and to evaluate whether this source model is valid as a representation of the blast. Parameters such as the detonation velocity, charge length and diameter have a direct link to the physical geometry. However, estimates of the pressure, the pressure load function, and the pressure rise-time were needed. A small amount of recorded data was available from three preconditioning experiments against which this source model could be tested (Rorke[12]). Each of these experiments recorded acceleration data at six positions close to a blast. One of the experiments consisted of a 61 mm diameter, 1.95 m blast hole detonated 4.75 m ahead of a tunnel, with propagation back toward the tunnel face. The array of accelerometers were mounted in a single plane, 3.7 m into the tunnel face (Figure 10). The physical parameters for the experiment were, 6 kg ANFEX, 1.95 m charge length, 0.06 m diameter and VOD = 3760 m/s, with measurements at 0.6 m, 1.2 m and 1.8 m from the axis of the blast.

Initial estimates of blast parameters were taken as 1 GPa peak pressure with a 100 μs rise-time. A model using these parameters gave amplitudes, which were 20 to 60 times less than the recorded velocities (Figure 11). Similar differences in amplitude were obtained when modelling the other two preconditioning experiments. Note that arrival times were not available from the data, and recorded waveforms have been shifted to coincide with the first arrival in the modelled waveforms.

In order to increase the modelled amplitudes, the options were to increase the pressure, decrease the rise-time, or increase the borehole diameter. It is important to note that the source was being modelled elastically. What was of interest were the seismic waves at a distance of many source radii from the borehole, and modelling detailed behaviour around the borehole such as fracturing needed to be avoided. Making the peak pressure too high was considered aphysical, while the measured waveforms did not indicate a faster rise-time. Other variations were attempted to account for the high amplitudes, including softening of the material around the blast.

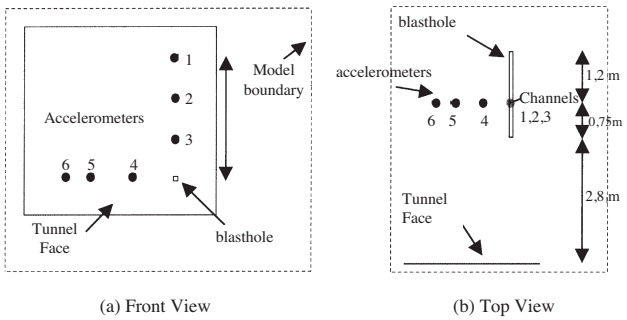

Figure 10—Model geometry for an earlier preconditioning experiment, showing positions of the blast hole, tunnel and accelerometer channels

A model was proposed where there is a much larger effective diameter, due to intense fracturing around the borehole and gas pressure propagating through these fractures. It was assumed that this causes a ring of pressure over a much larger diameter in the rockmass, and that this ring of pressure propagates with the detonation velocity. The gas propagation would also account for slower rise-times in pressure than would be expected at the wall of the borehole. In practice it is not possible to have an arbitrary source diameter as this needs to be an integral number of elements. The relationships described in the previous section allow the peak pressure to be fine-adjusted to give the same effect as the desired diameter.

Figure 12 compares results for three accelerometer positions. The model used a peak pressure of 3.1 GPa, a pressure rise-time of 100 μs, and an effective borehole diameter of 0.27 m. Other parameters were obtained directly from the physical blast parameters. The effective diameter was approximately 4.5 times the real diameter. The above approach was able to account for the measured amplitudes.

The other important aspect of the propagating blast model, is that a slow velocity of detonation produces high amplitude shear waves. The experiment had a detonation velocity close to the shear wave speed of the surrounding rock, but the number of waveforms was too limited to confirm or refute this result.

Calibration blast at the tunnel site

A calibration blast was made at the experimental tunnel site. This was used to test equipment and to provide data against

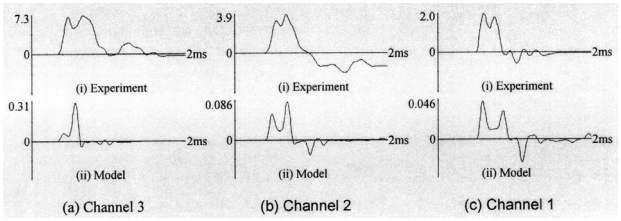

Figure 11—Velocity seismograms (in m/s) from the preconditioning experiment compared to those from the model with a source pressure of 1 GPa, a rise-time of 100 μs, and a borehole diameter of 0,06 m. Experimental waveforms were obtained by integrating accelerometer data, and arrivals have been shifted to correlate with the model (since absolute arrival times were not recorded). Channels 1 to 3 are respectively 1.8 m, 1,2 m and 0.6 m from the source. Note that modelled amplitudes are an order of magnitude lower than experimental values

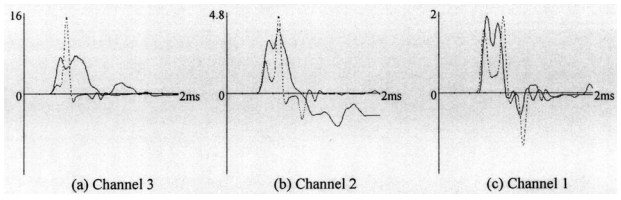

Figure 12—Velocity seismograms (in m/s) fromthe preconditioning experiment (solid) compared to the model (dotted) with a source pressure of 3.1 GPa, a rise-time of 100 μs, and a borehole diameter of 0.27 m (compared to a physical diameter of 0.06 m). Recorded arrivals were shifted to coincide with modelled arrivals

which to test the model. It consisted of a small blast in the tunnel wall at the opposite end of the tunnel from where the main blast was planned.

The geophones for the main experiment were in place for the calibration blast. Figure 13 shows the model of the tunnel site, position of the calibration blast and the position the geophones used in comparisons. The blast hole was drilled one metre into the tunnel wall at 75 degrees to the tunnel wall, with a diameter of 0.037 m. The charge length was 0.65 m, the charge mass 0.67 kg, and the detonation velocity 4500 m/s. Further details on the calibration experiment and equipment is given in Milev *et al.*[13].

The propagating source model was used, and the best match source parameters were a source rise-time of 800 μs, a peak pressure of 3.4 GPa, and an effective diameter of 0.21 m (5.7 times the physical diameter). The rise time was based on long pulse widths in the data, which differed significantly from data from the preconditioning experiment, where pulse widths are much shorter.

The modelled waveforms corresponded encouragingly with those measured from the calibration blast. Waveforms are compared in Figure 14a (observed) and b (modelled), for positions along the tunnel wall with motions normal to the tunnel wall. P- and S-wave arrivals are clearly visible. The waveforms, amplitudes and relative amplitudes of the P-wave to the S-wave are remarkably similar.

The wave-speeds calculated from the measured waveforms were surprisingly high, with a P- and S-wave speed of 7000 m/s and 4000 m/s respectively. Although there is an error margin of ±11% in the P-wave velocity and ±6% in the S-wave velocity, it is clear from Figure 14 that the real wave speeds are significantly faster than those of the model. The model wave speeds are 5740 m/s and 3514 m/s. These correspond to elastic parameters of Young's Modulus 80 GPa, Poisson's ratio 0.2 and density 2700 kg/m^3, considered typical for the region.

Triaxial data was recorded at two positions very close to the source and not all components from the model compared well. Geophone recordings shown in Figure 15 formed a triaxial set on the tunnel wall 1.7 m ahead of the blast, while geophones in Figure 16 formed a triaxial set mounted 5 m into the tunnel wall (i.e. in solid rock). The blasthole was modelled as truly horizontal. A significant departure from this in the real blast could account for large recorded vertical velocities (Y-vel in Figures).

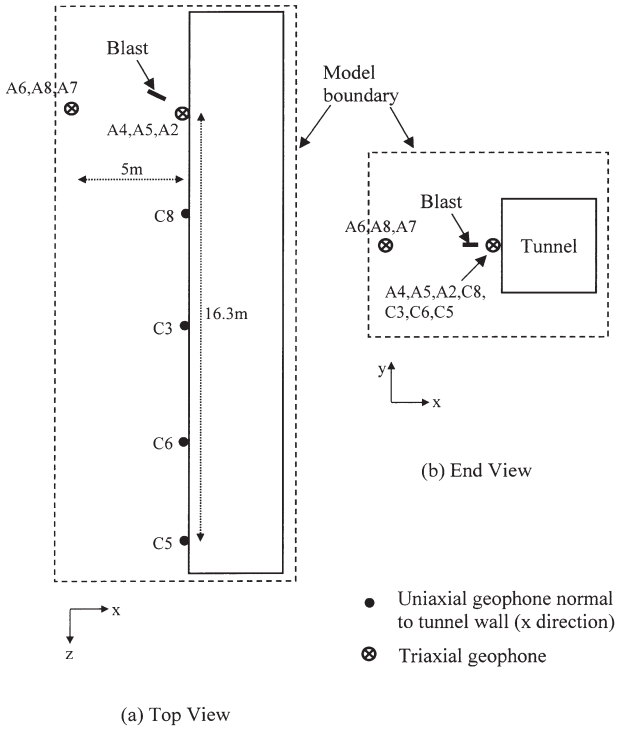

Figure 13—Schematic of the model geometry for the calibration experiment, showing the positions of the blast and the various geophones used in comparisons

Forward modelling of the main blast

The source for the rockburst experiment needed to approximate in certain aspects the loading from a near-field

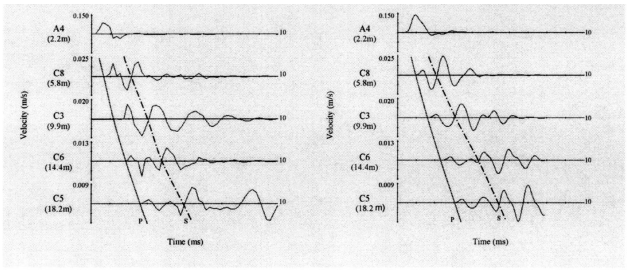

Figure 14—Comparison of velocity seismograms for the calibration blast at varying distances along the tunnel near wall. Positions for geophones A4, C8, C3, C6, C5, are shown in Figure 13. Motion is normal to the tunnel surface. Approximate P-wave arrivals and the position of the S-wave (not the S-wave arrival, are identified

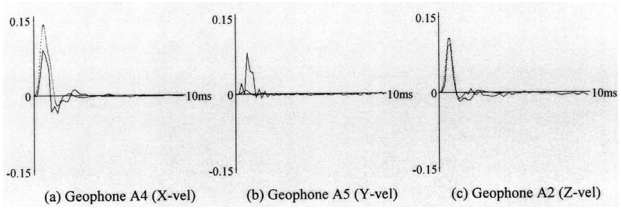

Figure 15—Recorded (solid) and modelled (dotted) velocity waveforms for the calibration blast, compared for geophones A4, A5 and A2, a triaxial set mounted on the tunnel wall 1.7 m ahead of the calibration blast

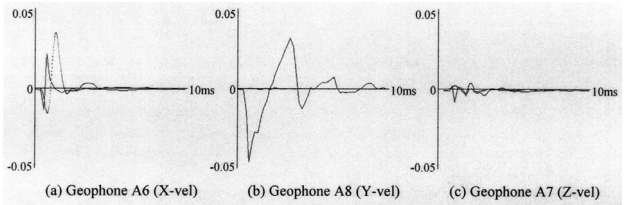

Figure 16—Recorded (solid) and modelled (dotted) velocity waveforms for the calibration blast, compared for geophones A6, A7 and A8, a triaxial set mounted 5 m into the tunnel wall in solid rock, 1.5 m ahead of the calibration blast

natural event. This meant that it should have a planar extent rather than emanate from a point and that waves should strike the tunnel obliquely. The effects of the blast itself, such as fracturing due to gas expansion, had to be isolated from the tunnel so that damage observed at the tunnel was due to seismic waves. However, the resulting seismic waves had to be large enough to cause visible damage. To satisfy these constraints, it was decided to use multiple blastholes parallel to the tunnel, each at a distance of 4 to 7 metres, with a charge length of 5 to 8 metres, and with some detonation velocity and charge mass.

Planning the experiment involved designing the blast in terms of size and timing, determining where damage was expected, positioning monitoring equipment, and tuning equipment to avoid saturation. This required estimates of the maximum velocity in the tunnel, the position of maximum motions and the rate of decay of motions along the tunnel. Forward modelling was able to give insight into the factors affecting these estimates. A reliable estimate of the actual maximum velocity was not feasible, as sources inferred from the two different sets of calibration data yield widely varying results.

Source parameters: Direct inference from the calibration data sets

Early on in the analysis, upper limits for the source parameters were proposed (Source #0). However, both sets of calibration data (the two previous sections) indicated that the model source requires far higher pressures than expected, or a greatly increased borehole diameter. A possible explanation is that crack growth from the borehole leads to the gas exerting pressure over a much greater 'effective' diameter in the rockmass. Since velocities scale with the square of the diameter (shown before), this would account for much larger velocities.

As a first approach to estimate realistic amplitudes, parameters for the source for the rockburst experiment were extrapolated from those used in the models of the preconditioning and the calibration blasts. A source (Source #1) was extrapolated from the model of the calibration experiment, by using the same peak pressure, rise-time and ratio of real to modelled borehole diameter. Similarly, Source #2 was extrapolated from the preconditioning experiment, by using its peak pressure, rise-time and ratio of real to modelled borehole diameter. Table I shows physical blast parameters and the best fit model parameters for the calibration and preconditioning experiment. It also shows four different projected sources for the rockburst experiment, and the projected maximum velocities at the tunnel from a single 6 metre long borehole of 0.1 m diameter. These velocities are for a single blasthole, whereas five blastholes were planned for the experiment and led to much higher velocities. The velocities from the sources differ considerably. Both Sources #1 and #2 gave what were considered unrealistically high velocities, although velocities from Source #2 from the calibration experiment were more in line with expected values.

Source parameters: Scaling effective diameter and amplitudes

The direct extrapolations given in the last section led to radically different projections for the tunnel velocity. An attempt was made to develop a rational basis for projecting source parameters which was consistent with both sets of calibration data. The model source parameters which affect amplitude are the detonation velocity, peak pressure, pressure rise-time, diameter and length (shown earlier). All but the diameter and rise-time can be related to physical blast parameters.

Pressure rise-times in models of the calibration experiments needed to be longer than expected. Long rise-

Table I

Physical blast parameters and model source parameters for the calibration and preconditioning experiment, and for four projections (source #0, #1, #2, #3) for the rockburst experiment. (M is the charge mass, L the charge length, M_L the charge per unit length, D the physical borehole diameter, VOD the velocity of detonation, D_{eff} the effective diameter, P the pressure, T the rise-time). Source #0 is based on initial assumptions. Source #1 is based on the calibration experiment model using its ratio of effective to real diameter. Source #2 is based on the preconditioning experiment model using its ratio of effective to real diameter. Source #3 is based on a power-law of 0.7 relating effective diameter to real diameter. The final row compares the maximum tunnel velocity predicted by the different projected sources, based on a single 6 metre blasthole parallel to the tunnel. V_{T5} is for a tunnel 5 metres from the blast, and $V_{T6.4}$ is for a tunnel 6.4 metres from the blast

	Symbol	Units	Calibr. expt.	Precon. expt.	Source #0	Source #1	Source #2	Source #3
	M	(kg)	0.66	6	54	54	54	54
Blast	L	(m)	0.65	1.95	6	6	6	6
(Physical	M_L	(kg/m)	1.02	3.08	9.0	9.0	9.0	9.0
parameters)	D	(m)	0.037	0.06	0.102	0.102	0.102	0.102
	VOD	(m/s)	4500	3760	4000	4000	4000	4000
Model	D_{eff}	(m)	0.206	0.274	0.102	0.57	0.47	0.42
(Effective	D_{eff}:D		5.57	4.57	1.0	5.57	4.57	4.13
parameters	P	(GPa)	3.41	3.1	3.1	3.1	3.1	3.1
	T	(Ms)	1200	150	200	1200	150	800
	PD_{eff}^2	(GPa m^2)	0.145	0.233	0.01	1.0	0.67	0.55
Projected	V_{T5}	(m/s)			0.11	2.0	8.3	1.6
Velocity at	$V_{T6.4}$	(m/s)			0.08	1.4	6.1	1.1

times could be explained by the time taken for cracks to grow and for gas pressure to propagate from the initial borehole diameter to the distance of the effective diameter. Table II shows the average pressure propagation speeds which would be required to give different rise-times. The optimum rise-times and hence the propagation speeds in the two calibration models, vary widely. A rise-time of 800 μs was projected for the rockburst experiment. This is in-between the two sets of calibration data but closest to the calibration experiment. Preference was given to the calibration experiment data as it took place at the same tunnel site, with the same measuring equipment as the main experiment.

From Table I it can be seen that for the best fit models for the calibration and preconditioning data, the effective diameter should not increase linearly with charge mass or charge diameter. The limited data suggests that, as charge mass or blast hole diameter increase, the relative increase in effective diameter (and crack extent) becomes less. The effective diameter was assumed to be a power of the real borehole diameter (i.e. $D_{eff} \propto D^{B}$, where B is a constant). More strictly one may expect it to be the increase in diameter which relates to the diameter, but for the range of interest and accuracy it is simpler to consider the above relationship (*cf*. Appendix A).

Table II projects effective diameters for the preconditioning and rockburst experiments based on the calibration experiment and different power laws. The bold values are those used in the best-fit models and correspond to a power law of $D_{eff} \propto D^{0.7}$. Appendix A shows that if the pressure rise-time is assumed to be constant (i.e. independent of blast size), then the effective diameter can be related to the charge mass and velocity. The power law ($D_{eff} \propto D^{0.7}$) leads to $D_{eff} \propto M_L^{0.35}$ and $v \propto M_L^{0.7}$, (where D_{eff} is the effective borehole diameter, D the initial borehole diameter, M_L the charge mass per unit length, and v the velocity at some distance from the blast). This velocity-mass relationship corresponds to an empirical relationship developed by Ouchterlony *et al.*[14]. A power law of $D_{eff} \propto D^{0.5}$ corresponds to $v \propto M_L^{0.5}$, which would imply a direct relationship between charge mass and kinetic energy at a point. Sources #1 and #2 given before, which produced what were considered to be unrealistically high velocities, were effectively based on a power law of $D_{eff} \propto D^{1}$.

Table I shows the physical and model parameters for the final projection (Source #3) for the rockburst experiment. The effective parameters are the calculated parameters, with the effective diameter based on a power law of $D^{0.7}$. In practice the actual diameter used in the model was dictated by the grid size and the pressure was adjusted according to the square of the diameter (*cf*. an earlier section) to give the same velocities. This approach was validated by using diameters both smaller and larger than the desired diameter.

A relationship has been suggested which relates charge-mass to the effective diameter and to velocity, and fits the limited cases studied. This assumes that the rise-times are similar for different size blasts. More data would be needed to develop a relationship which couples both the rise-time and the effective diameter.

Position of maximum velocity at the tunnel

The original models were based on a blast design for an 8 metre blasthole, parallel to the tunnel and 5 metres into the solid. The models presented here were updated after the experiment for a 6 metre blasthole at a distance of 6.4 metres, which is closer to the actual blast geometry. Results are qualitatively consistent with the earlier models.

The source parameters of Table I (Source #3) were used to model a single 6 metre long blasthole, with a 54 kg charge mass and a detonation velocity of 4000 m/s. This produced a maximum tunnel velocity of 1.1 m/s located 5 metres ahead of the blasthole. The velocity decays to half the maximum value 12 metres ahead of the blast. Figure 17a shows the velocity distribution on the near tunnel wall, and the projection of the blastholes (which are 6.4 metres from the tunnel).

The models show two influences on the position of maximum velocity at the tunnel, namely the detonation velocity and the rise-time. This is in accordance with the radiation patterns previous. Increasing the detonation velocity (Figure 17b) shifts the position of the maximum velocity back towards the blast. Similarly, a 50% longer rise-time (Figure 17c) shifts the maximum velocity backwards such that it is opposite the end of the blasthole.

Results of the modelling encouraged choosing a low detonation velocity (i.e. 4000 m/s) for the blast as it

Table II

'Effective diameters' based on the model source from the calibration experiment and projected for the preconditioning and rockburst experiments using three different power laws. (D is the real borehole diameter. D_{eff} the effective diameter)

	Calibration experiment	Precon. experiment	Rockburst experiment
D	0.037	0.060	0.102
$D_{eff} = 5.6*D^{1}$	0.21	0.34	0.57
$D_{eff} = 2.075*D^{0.7}$	**0.21**	**0.29**	**0.42**
$D_{eff} = 1.075*D^{0.5}$	0.21	0.26	0.34

Table III

Relationship between source rise-time and crack and gas pressure propagation, assuming that the source rise-time results from propagation to a distance of the effective diameter. Average speeds for crack and gas pressure propagation (C_{CR}), are shown for the three different rise-times inferred for models of the three experiments. (D is the initial borehole diameter, D_{eff} the effective diameter, C_L the length of cracking, C_P the P-wave speed, C_{CR} the average crack growth and gas propagation speed)

	Units	Calibration experiment	Precon. experiment	Rockburst experiment
D	(m)	0.037	0.060	0.102
D_{eff}	(m)	0.21	0.29	0.42
C_L	(m)	0.085	0.115	0.159
C_P	(m/s)	5800	5800	5800
T	(μs)	1200	150	800
C_{CR}	(m/s)	70	614	192

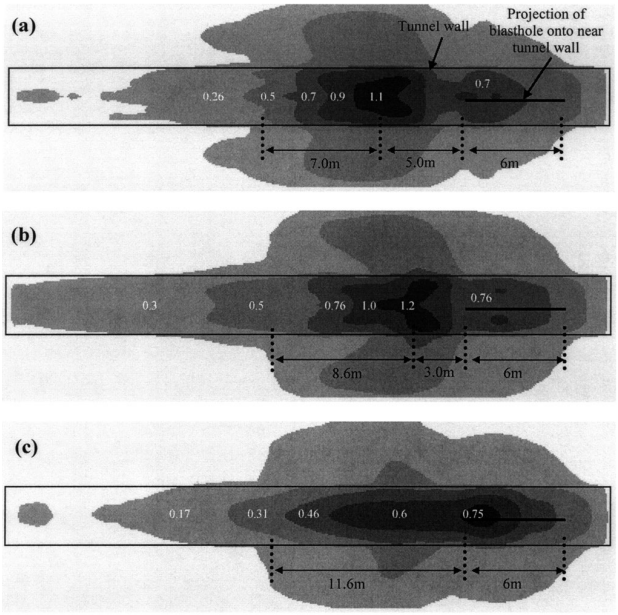

Figure 17—Projected maximum velocity (in m/s) on the tunnel near-wall, for a single 6 metre blasthole, with source parameters in Table I (Source #3) (a) VOD = 4000 m/s, T = 800 μs (b) VOD = 5000 m/s. T = 800 μs (c) VOD = 4000 m/s, T = 1200 μs

predicted greater shear wave generation. From the modelling results, the position of the maximum could be ahead of the blast. In the final experiment, accelerometers were positioned on the tunnel wall, opposite and 3 metres ahead of the blast to ensure that the maximum velocity was measured.

Multiple blasts

Five separate blastholes were planned for the experiment, to generate sufficiently large seismic waves. Figure 18 shows the velocity distribution on the tunnel near wall for the model of the blasts. These were spaced at 0.4 metre intervals and sequenced from bottom to top with a delay of 0.1ms. (These delays give a propagation velocity equal to the detonation velocity, i.e. 4000 m/s). The maximum was 6 m/s which is more than 5 times the peak velocity for a single blasthole. (This is possible since the model is not a superposition of five blasts.) Different blast delays were studied, and larger delays led to significantly lower velocities.

Discussion

The main purpose of this work was to gain understanding of what motions could be expected at the tunnel in the main experiment. In the process, a number of insights have also been gained on wave propagation from a propagating blast and the numerical representation of this.

A propagating pressure along the surface of a borehole, is thought to be an appropriate representation of a blast propagating with a finite detonation velocity. A numerical source was developed and shown to give equivalent results to the analytical solution to a pressure propagating inside a circular borehole. It was shown that the waves emanating from such a source can be modelled sufficiently accurately in a finite difference program, without modelling the borehole surface and with an element size of the same order as the borehole diameter. Scaling rules were developed such that a diameter larger than the physical diameter could be used in the model. In particular, distant velocities scale with the square of the borehole diameter. This is very important from the point of view of numerical efficiency, when the distances being considered are much greater than the borehole diameter.

The analytic result is valid only for a detonation velocity greater than the P-wave speed. The numerical results are assumed to be valid for any detonation velocity, and have given insights for lower detonation velocities. The source produces both P- and S-waves, and for low detonation velocities approaching the shear wave velocity, the amplitude of the S-waves are much larger than the P-waves. The relationship of peak pressure, pressure rise-time, and borehole diameter to the amplitudes of the velocities was studied. The detonation velocity and pressure rise-time proved to have an important influence on the radiation pattern, in terms of how far the maximum velocities are skewed ahead of the blast.

A very important result is that physical velocities measured at a distance from propagating blasts are an order of magnitude higher than those generated by this source model using the physical diameter. It has been argued that this could be due to the cracking process leading to the gas exerting pressure over a much larger volume. Crack and gas propagation would also explain the relatively long rise-times in the experimental waveforms.

Brady and Brown[15] describe three zones around a blasthole. A shock zone of up to 2 diameters; a transition zone of 4 to 6 diameters which is a non-linear elastic zone with large strain; and a seismic zone which is a linear elastic region, although crack extension may occur up to 9 diameters. The influence of this cracking makes it difficult to predict what waves occur beyond the fractured region. It was proposed that the same source (i.e. a borehole with a propagating pressure) could be used, but with a larger diameter, where the 'effective' diameter relates to the distance over which extensive cracking occurs. The pressure is applied to a ring surrounding the cracked region and propagates at the same rate as the detonation velocity. The pressure rise-time is considerably longer than would be expected at the surface of the actual borehole, due to the need for the cracks and gas to propagate to that distance. A method of scaling the effective diameter to charge mass was suggested. However, this was based on very limited data, and the method does not take into account the amplitude effects of changes in the pressure rise-time.

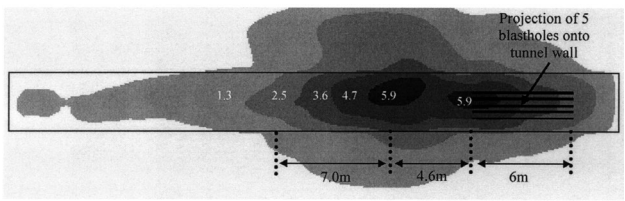

Figure 18—Projected maximum velocity (in m/s) on the tunnel near-wall, for five blastholes, each 6 metres long, with source parameters in Table I (Source #3). The blastholes had a 0.4 m spacing, and were synchronized from bottom to top with a delay of 100 μs, VOD = 4000 m/s, T = 800 μs, as for figure 17(a)

A detonation pressure (3 GPa for the ANFO blasts) was used as the peak pressure for the model, requiring effective diameters of 4 to 6 times to give the measured wave amplitudes. Such pressures would still lead to intense fracturing. It may therefore seem more appropriate to increase the diameter further and to decrease the peak pressure. It has been indicated that for sufficient distances, peak pressure and borehole diameter can be altered interchangeably in the model. Multiple blastholes complicate the choice of effective diameter, as these can merge to form a much larger diameter, in which case the tunnel is not far enough for the pressure-diameter scaling law to hold. Donzé and Magnier.[10] describe a model of an explosive source which demonstrates that higher amplitudes can occur due to the fracturing process, compared to an homogeneous elastic medium. It seems reasonable therefore to use an effective diameter based on the extent of the non-linear region, with a higher than physical pressure in an elastic representation of the source.

For the detonation velocities considered, the source model predicts that the shear waves generated have much greater amplitudes than the P-waves. Comparisons of the models with calibration data did not confirm this. Data was also insufficient to reject this prediction. If work with propagating explosions is pursued in the future, it is recommended that experiments be made to establish whether the blast does indeed generate significant shear waves.

Models of the calibration experiment were particularly encouraging and waveforms for many positions corresponded well in first motions and amplitudes, with many corresponding well with the overall waveforms. This gives confirmation that the model can realistically model the wave propagation in the vicinity of the tunnel and the influence of the free surface—at least for small amplitude waves, and relatively unfractured tunnel walls.

Appropriate values for source parameters, such as pressure rise-time and effective diameter, were projected for the experiment based on the available data. Others such as peak pressure, detonation velocity and charge length, had a direct relationship to the physical blast design. Projections of the motions at the tunnel surface were made for the final experiment. The model predicted that the detonation velocity and the rise-time had a very significant influence on the position where the maximum motions in the tunnel could be expected. For the planned detonation velocity of 4000 m/s, the model predicted that the maximum tunnel velocity would be ahead of the blast for short rise-times but opposite the blast-holes for longer rise-times. Modelling also showed that the wave amplitudes at the tunnel would be much higher for multiple blastholes compared to a single blast, but only if the blasts were well synchronized. Models of the final rockburst experiment and comparisons with the experimental observations are presented in a related paper, Hildyard and Milev[16].

Conclusions

A number of important results were obtained and are summarized below.

- The implications of the described model of a propagating blast are that the rate of detonation should have an effect on the relative content of P- and S-waves and on the position where maximum velocity is to be expected at the tunnel
- The effects of various parameters in the blast model were studied. One important result was that velocity at a distance is proportional to the square of the diameter
- The simple application of a pressure and the physical borehole diameter leads to much lower velocities than those measured. A larger effective diameter based on a region of cracking was proposed to account for this behaviour
- Measured waveforms indicate that the velocities of the rock around the tunnel site are high compared to those normally expected
- The calibration blast model compared well enough with the data to indicate that realistic motions around the tunnel can in principle be modelled
- Comparisons with the calibration data were not sufficient to validate the appropriateness of the propagating source as a model for a detonating blast.

Acknowledgements

The modelling and developments in this paper have been performed whilst the first author pursued a Ph.D. degree at Keele University and Liverpool University in the United Kingdom, under the supervision of Professor R.P. Young, on the subject of seismic wave interaction with underground openings. The authors have also had useful discussions with Dr N. Kouzniak, Dr S.M. Spottiswoode, Dr J.A.L. Napier and Prof. R.P. Young. This work is supported under the project GAP 601, at the CSIR Division of Mining Technology, and is sponsored by SIMRAC (Safety in Mines Research Advisory Committee). This sponsorship is gratefully acknowledged. The Rockburst experiment was conducted, under the project GAP 530, by the CSIR Division of Mining Technology in 1998. Again sponsorship by SIMRAC is gratefully acknowledged.

References

1. Hagan, T.O., Milev, A.M., Spottiswoode, S.M., Hildyard, M.W., Grodner M.W., Rorke, A.J., Finnie, G.J., Reddy, N., Haile, A.T., Le Bron, K.B., and Grave, D.M. Simulated rockburst experiment—an overview. Journal of The South African Institute of Mining and Metallurgy, 2001, submitted.
2. Cundall, P.A. 'Theoretical basis of the program WAVE'. Unpublished internal report, COMRO (now Miningtek, CSIR, South Africa), 1992, 1–12 pp.
3. Hildyard, M.W., Daehnke, A., and Cundall, P.A. WAVE : A computer program for investigating elastodynamic issues in mining. *Procs. of the 35th US Symposium on Rock Mechanics*, Reno, Nevada, June 1995. AA Balkema, Rotterdam.
4. Parnes, R. Response of an infinite elastic medium to travelling loads in a cylindrical bore. *J. Appl. Mech*., 1969, vol. 36, pp. 51–58.
5. Daehnke, A. Stress wave and fracture propagation in rock. Ph.D. thesis, Vienna University of Technology, 1997, 408 pp.
6. Kouzniak, N. and Rossmanith, H.P. Supersonic detonation in rock mass - Analytical solutions and validation of numerical models—Part 1: Stress analysis. *FRAGBLAST—Int. J. of Blasting and Fragmentation*, 1998, vol. 2, no. 4, pp. 449–486.
7. Rossmanith, H.P., Uenishi, K., and Kouzniak, N. Blast wave propagation in rock mass—Part I: monolithic medium. *FRAGBLAST—Int. J. of Blasting and Fragmentation* 1, 1997, pp. 317–359.
8. Uenishi, K. and Rossmanith, H.P. Blast wave propagation in rock mass—Part II: layered media. *FRAGBLAST—Int. J. of Blasting and Fragmentation* 2, 1998, pp. 39–77.

9. Denny, M.D. and Lane, R.J. The explosion seismic source function: models and scaling laws reviewed, in *Explosion Source Phenomenology, Geophysical Monograph* vol. 65, ed. Taylor *et al*, pp. 1–24, AGU, Washington DC, 1991.
10. Donze, F. and Magnier, S.A. Numerical modelling of a highly explosive source in an elastic-brittle rock mass. *J. Geoph. Res.*, 1996, vol. 101, B2, Feb 10, pp. 3103–3112.
11. Timoshenko, S.P. and Goodier, J.N. *Theory of Elasticity*, 3rd Ed., McGraw-Hill, 1970.
12. Rorke, A.J. Measurement of the direct effects of preconditioning blasts. Monitored results from the first test blast. Internal report, prepared for D. Adams, Feb 1992, COMRO, Ref R62/92.
13. Milev, A.M., Spottiswoode, S.M., Rorke, A.J., and Finnie, G.J. Seismic monitoring of a simulated rockburst on a wall of an underground tunnel. The Journal of The South African Institute of Mining and Metallurgy, 2001, submitted.
14. Ouchterlony, S.N., Nyberg, U., and Deng, J. Monitoring of large open cut rounds by VOD, PPV and gas pressure measurements. *Fragblast International Journal of Blasting and Fragmentation*, vol. 1. , no. 1, 1997 pp 3–25.
15. Brady, B.H.G. and Brown, E.T. *Rock mechanics for underground mining*. 2nd ed, Chapman and Hall, London, 1993, pp. 466–475.
16. Hildyard, M.W. and Milev, A.M. Simulated rockburst experiment: Numerical back-analysis of seismic wave interaction with the tunnel. The Journal of The South African Institute of Mining and Metallurgy, 2001, submitted.

Appendix A: Scaling the source (effective diameter) to the charge mass

The following argument attempts to provide some basis for the choice of the effective diameter. Define C_L as the length of cracking around the borehole, D_{eff} as the effective borehole diameter, D the initial borehole diameter, M_L the charge mass per unit length, V the charge volume, L the charge length, and v the velocity at some distance from the blast. Assume also that the pressure rise-time is constant, i.e. independent of blast size.

By definition,

$$D_{eff} = D + 2C_L \quad [1]$$

Assume the increase in diameter is related to the physical diameter by a power law,

$$D_{eff} = D + A'D^{B'} \quad [2]$$

where A' and B' are constants. For the range of interest (*cf.* Table I), D_{eff} is much larger than D, and we can assume a simpler relationship which relates the effective diameter to the real diameter,

$$D_{eff} \propto D^B \quad [3]$$

where B is constant. Now, for the same density of charge,

$$M_L \propto V / L \propto D^2 \quad [4]$$

and hence the effective diameter is related to the charge mass per unit length by

$$D_{eff} \propto M_L^{B/2} \quad [5]$$

From the third section, provided that other source parameters such as peak pressure, rise-time, length, and velocity of detonation, are unchanged, then the velocity at a point is proportional to the square of the modelled diameter, i.e.

$$v \propto D_{eff}^2 \quad [6]$$

and hence from [5] and [6]

$$v \propto M_L^B \quad [7]$$

In this paper we have used a power law of $D_{eff} \propto D^{0.7}$ (i.e. B = 0.7), which gives the relationship $D_{eff} \propto M_L^{0.35}$, and leads to $v \propto M_L^{0.7}$. This is the same as the empirical velocity-mass relationship developed by Ouchterlony *et al.*[14]. A law of $D_{eff} \propto D^{0.5}$ leads to $v \propto M_L^{0.5}$, while a law of $D_{eff} \propto D^1$ leads to $v \propto M_L$. ◆

New technology demonstration centre at Mintek*

A new technology demonstration centre called ZenZele (ZenZele = the Zulu word for self reliance), which will assist artisanal and small-scale miners to develop processes to get their operations started, is being set up at Mintek, after successful application for funding from the Department of Arts, Culture, Science and Technology, the Department of Trade and Industry, and other stakeholders, assured a grant to carry the project over the next three years.

According to Mintek's Manager; Minerals Processing, Rob Guest, Mintek applied for this grant because of its grass roots involvement in training of small-scale miners over the years.

'It is planned to assist these small operators assess their deposits; research the best methods for the extraction of the minerals; source equipment and build plants; draw up business plans, and, in this way, establish between 40–50 small to medium fully-functional enterprises, each employing a couple of hundred people, in various rural areas.'

The ZenZele project will also be hosting a series of workshops and seminars around the country, at the same time as going out into the field to assess likely deposits. ◆

* *Contact: Rob Guest Tel: (011) 709-4445, or Dr Colin Logan, Tel: (011) 709-4429*

Urgent action required on metallurgical accounting*

—Cape Town workshop calls for industry standard

A mineral processing workshop held in Cape Town during August, 2001, has identified the pressing need for an industry-wide standard in metallurgical accounting.

The SAIMM 'Challenges in Metallurgical Accounting and Information Management' workshop identified for urgent attention the largely unaccounted factor of comparing metal-out against metal-in at a typical processing or smelting operation.

AMIRA International research coordinator Mr Richard Beck said a problem for many mining and processing operations was to get a balance at the end of each month, particularly in smelters and hydrometallurgical plants where it isn't easy to sample intermediate products.

'You get stockpiles of material building up in inventory which are very difficult to quantify,' he said. 'Most smelters work on an accounted loss as a matter of course, the size of the accounted loss being an established industry figure—which for any financial accountant would be unthinkable.'

He said many operations measured the amount of metal in feed and waste streams stating recovered metal as the difference: 'But the metal going out isn't actually measured compared with the metal coming in—the true recovery is metal out against metal in.

'Fundamentally the metallurgist wants to know what the exact answer is and if supplied with the right tools to help trace these things, then there would be major advantages.'

Mr Beck said AMIRA would aim to set up a collaborative project to draw up a standard set of metallurgical accounting practices for the mining industry.

'The industry should lead the way, which is why research organizations like the Julius Kruttschnitt Mineral Research Centre should be involved through their expertise in statistical analysis, ore handling, milling, sampling and the mine-to-mill research approach.

'Whatever comes out of this must be practical and under friendly to suit a particular operation irrespective of size, scale and type of metal produced.'

JKMRC Director Professor Tim Napier-Munn said the JK Centre was ideally placed to make a significant contribution towards any adoption of a metallurgical accounting standard for the global minerals industry.

Professor Napier-Munn said the JKMRC has already developed the potential 'tool of choice' in JKMetAccount as the metallurgical accounting package that would help provide a standardized approach for the industry to follow.

He said, the JKMRC had taken the initiative during the 1990s to draw its experience in statistical analysis, mass balancing and plant optimization together into one comprehensive metallurgical accounting package.

Given the current problem in providing uniform data across complex processing operations, JKMetAccount can be used to reconcile concentrator production with ore supplied from multiple sources.

Professor Napier-Munn said the JKMRC's commercial division JKTech Pty Ltd could be called upon to help those operations needing assistance with any future move towards an industry-led and controlled metallurgical accounting standard.

Mr Beck said the main advantage from having a metallurgical accounting standard, supported by a tool such as JKMetAccount, would be to give operators an approach to do things better in the plant.

'Metallurgical balancing around plants has been notoriously difficult.'

He added any company involved in toll refining would also be considerably advantaged with a new standard.

'Toll refining—where a refiner buys in concentrates or intermediate products from one place to another—is even starting to happen within companies which are treating various parts of their operations as business units, apportioning costs to different sections.

'If you are in the toll refining business you really need to know what to do, and is an area where there is likely to be intense interest in a met accounting standard, either with other people or in-house.'

Workshop chairman UCT Associate Professor Gaylard said drafting a set of guiding principles for metallurgists to follow would eventually be required by company shareholders.

He said such a standard for assessing metallurgical performance had not existed mainly because each operation applies different processes to different metals and grades of ore: 'But that doesn't mean there can't be a set of basic guiding principles to follow.'

In terms of corporate governance, Professor Gaylard says more could be done to teach young metallurgists and mining engineers about the significance of metal accounting.

'When a mine is floated, shareholders are told what the company believes the orebody contains, but after mining shareholders are told about the amount of metal processed—there is no balancing back to what was originally stated to be in the orebody.

'This is where tighter metallurgical accounting has a role.'

For further information contact:

Dr Rob Morrison, JKMRC Technical Director:
Tel: +61 7 33655843, Fax: +61 7 33655999,
Email: r.morrison@uq.edu.au
Mr David Stribley, Group Leader: Mineral Processing Business Unit AMIRA International: Tel: +613 9679 9976, Fax: +61 3 96799900 Email: david.stribley@amira.com.au
Mr Richard Beck, AMIRA Research Coordinator, Johannesburg: Tel: +27 11 4651601, Fax: +27 11 4651068, Email: richard.beck@amira.com.au
Associate Professor Peter Gaylard, Department of Chemical Engineering, University of Cape Town: Tel/Fax: +27 21 6860256, Email: pgaylard@chemeng.uct.ca.za ◆

---

* *Contact: David Goeldner, JKMRC Communications Coordinator, Tel: +61 7 3365 5848, Email: d.goeldner@uq.edu.au*